Pergamon

0301-9322(94)00080-8

Int. J. Multiphase Flow Vol. 21, No. 3, pp. 501–513, 1995

0301-9322/95 $9.50 + 0.00

GRAVITY-DRIVEN TWO-LAYER FLOW DOWN A SLIGHTLY WAVY PERIODIC INCLINE AT LOW REYNOLDS NUMBERS

FENG KANG and KANGPING CHEN

Department of Mechanical and Aerospace Engineering, Arizona State University, Tempe, AZ 85287, U.S.A.

(Received 10 October 1993; in revised form 2 November 1994)

Abstract—Gravity-driven two-layer flow down a slightly wavy periodic incline at low Reynolds numbers is studied by a perturbation approach. Amplitude ratios and phase shifts of the fluid–fluid interface and the fluid–air free surface relative to the wavy wall are obtained as functions of the incline angle, wavelength of the roughness, and the ratios of film mean thickness, density and viscosity. Effects of surface tension and interface are included, and wall-shear-stress distributions are also discussed.

Key Words: low Reynolds number flow, thin films, wavy wall

1. INTRODUCTION

Multilayer flows of immiscible viscous fluids are frequently encountered in many industrial processes. Examples of these processes include multiple layer coating and coextrusion of polymeric materials. To ensure the quality of the products manufactured by these processes, it is very often desirable to maintain the thickness of each layer uniform during the process. Thus the stability of the uniformly layered flow is essential for the success of these operations. The stabilities of uniformly layered flows in different simple geometries have been extensively studied in the past decade, and the recent monograph of Joseph & Renardy (1993) gives a comprehensive summary of these studies.

Gravity-driven flow of liquid films down an inclined plane has been used as a prototype problem for the study of coating flows. Stability for a single Newtonian layer has been investigated by Yih (1954, 1963), Benjamin (1957) and many others (see Lin & Wang 1985 for a review for the literature prior to 1985, and Joo & Davis 1992, for the most recent developments). Stability of multiple layer flows has also been considered by many people (Kao 1965a, b, 1968; Wang *et al.* 1978; Lin 1983; Loewenherz & Lawrence 1989; Weinstein 1990; Weinstein & Kurz 1992; Chen 1993). All of these studies are restricted to the situation in which the inclined plane is perfectly smooth. In coating operations, the substrate can be inclined to the horizontal after the fluid layers are coated on the substrate. It is of interest to study the effect the roughness of the substrate may have on the film uniformness. In the case of small roughness; one may approximate the incline as a periodic sinusoidal surface with a small amplitude. Multiple film over a wavy surface may also be of interest to other applications, such as flow through trickle-bed reactor and porous media (Dassori *et al.* 1984; Santos *et al.* 1991).

Steady low Reynolds number flow of a Newtonian liquid layer down a slightly wavy surface has been considered by Wang (1981) by means of a perturbation analysis. Pozrikidis (1988) extended Wang's study to the case of large waviness using a boundary integral method. Tougou (1978) has considered the long wave stability of these flows. In this paper, we consider the steady flow of two liquid layers, assuming small waviness of the inclined plane. Whether steady flow can be achieved depends on the residence time of the fluid on the incline and the wavelength of the roughness. Thus the steady state analysis presented here is only appropriate under certain conditions. A perturbation analysis is performed for small Reynolds number flow. The effects of the wall roughness on the film thickness variations as well as other characteristics of the perturbed flow will be discussed.

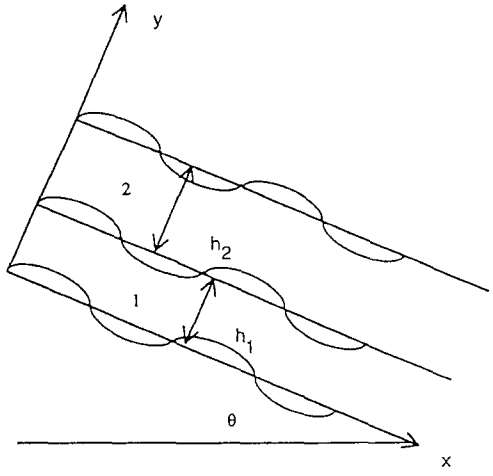

Figure 1. Flow configuration.

2. MATHEMATICAL FORMULATION

Consider gravity-driven laminar flow of two viscous, incompressible fluids down a slightly wavy incline, as shown in figure 1. The origin of the y-axis is placed on the mean position of the incline, which forms an angle θ with the horizontal. The x-axis is in the direction of the mean flow. The mean thickness of each fluid layer is h_i, $i = 1, 2$, for the bottom and the top layer, respectively. The problem can be formulated in dimensionless form by choosing appropriate scales. We shall use the mean thickness of the bottom layer, h_1, as the length scale, the mean velocity of the interface, U, as the velocity scale and h_1/U as the time scale. The dimensionless wavy incline is given by $y = \epsilon \sin(\alpha x)$, where ϵ is the dimensionless amplitude and $2\pi/\alpha$ is the dimensionless wavelength.

In this study, we shall restrict attention to the small waviness case, in which the amplitude of the wavy incline is small compared to the mean thickness of the bottom layer, $\epsilon \ll 1$. The fluid–fluid interface is given by $y = 1 + f(x; \epsilon)$. The fluid–air free surface is given by $y = 1 + n + g(x; \epsilon)$, where $n = h_2/h_1$ is the ratio of the mean thickness of the top layer to that of the bottom layer.

The dimensionless continuity and momentum balance equations for two-dimensional steady flow in each layer, $i = 1, 2$, are

$$\frac{\partial u}{\partial x} + \frac{\partial v}{\partial y} = 0, \qquad [1]$$

$$\mathrm{Re}\left(u\frac{\partial u}{\partial x} + v\frac{\partial u}{\partial y}\right) = -\frac{\partial p}{\partial x} + G_x + \Delta u, \qquad [2]$$

$$\mathrm{Re}\left(u\frac{\partial v}{\partial x} + v\frac{\partial v}{\partial y}\right) = -\frac{\partial p}{\partial y} + G_y + \Delta v, \qquad [3]$$

where $\mathrm{Re}_i = Uh_1\rho_i/\eta_i$, $i = 1, 2$, are the Reynolds numbers for each layer, $G_{xi} = \rho_i h_1^2 \boldsymbol{g} \sin\theta/U\eta_i$, $G_{yi} = -\rho_i h_1^2 \boldsymbol{g} \cos\theta/U\eta_i$, and Δ is the two-dimensional Laplacian. ρ_i, η_i, $i = 1, 2$, are the densities and viscosities of the two fluids.

On the wavy inclined plane $y = \epsilon \sin(\alpha x)$, no-slip condition applies:

$$u = v = 0. \qquad [4]$$

On the fluid–fluid interface $y = 1 + f(x; \epsilon)$, we have the kinematic condition

$$v = u\frac{\partial f}{\partial x}. \qquad [5]$$

The continuity of velocity requires

$$\|u\| = 0, \tag{6}$$

$$\|v\| = 0, \tag{7}$$

where $\|F\| = (F)_1 - (F)_2$ is the jump in F across the interface. The tangential stress and normal stress balance equations are

$$\left[1 - \left(\frac{\partial f}{\partial x}\right)^2\right] \left\| m\left(\frac{\partial u}{\partial y} + \frac{\partial v}{\partial x}\right) \right\| + 2\frac{\partial f}{\partial x} \left\| m\left(\frac{\partial v}{\partial y} - \frac{\partial u}{\partial x}\right) \right\| = 0, \tag{8}$$

$$-\|mp\| + 2\left\{\frac{\partial f}{\partial x} \left\| m\left(\frac{\partial u}{\partial y} + \frac{\partial v}{\partial x}\right) \right\| + \left(\frac{\partial f}{\partial x}\right)^2 \left\| m\frac{\partial u}{\partial x} \right\| + \left\| m\frac{\partial v}{\partial y} \right\|\right\} \Big/ \left[1 + \left(\frac{\partial f}{\partial x}\right)^2\right] - \sigma_1 \frac{\partial^2 f}{\partial x^2} \Big/ \left[1 + \left(\frac{\partial f}{\partial x}\right)^2\right]^{3/2} = 0, \tag{9}$$

where $m = \eta_2/\eta_1$, and σ_1 is the dimensionless interface tension, $\sigma_1 = \sigma_1^*/\eta_1 U$. The top layer is assumed to be adjacent to passive air. On the fluid–air free surface, $y = 1 + n + g(x;\epsilon)$, we have the kinematic condition

$$v = u\frac{\partial g}{\partial x}. \tag{10}$$

The tangential stress vanishes

$$\left[1 - \left(\frac{\partial g}{\partial x}\right)^2\right]\left(\frac{\partial u}{\partial y} + \frac{\partial v}{\partial x}\right) + 2\frac{\partial g}{\partial x}\left(\frac{\partial v}{\partial y} - \frac{\partial u}{\partial x}\right) = 0. \tag{11}$$

and the normal stress balances the surface tension force

$$-p + 2\left\{\frac{\partial g}{\partial x}\left(\frac{\partial u}{\partial y} + \frac{\partial v}{\partial x}\right) + \left(\frac{\partial g}{\partial x}\right)^2\left(\frac{\partial u}{\partial x}\right) + \frac{\partial v}{\partial y}\right\} \Big/ \left[1 + \left(\frac{\partial g}{\partial x}\right)^2\right] - \sigma_2 \frac{\partial^2 g}{\partial x^2} \Big/ \left[1 + \left(\frac{\partial g}{\partial x}\right)^2\right]^{3/2} = 0, \tag{12}$$

where σ_2 is the dimensionless surface tension, $\sigma_2 = \sigma_2^*/\eta_2 U$. The pressure of the passive air has been taken as zero.

When the waviness of the incline is small and the flow is slow, the boundary-value problem [1]–[12] can be solved by a regular perturbation procedure (Wang 1981). Particularly, the governing equations can be solved explicitly when the Reynolds numbers of each layer are both of order ϵ. We shall restrict ourselves to these simple cases. All the variables in each region are expanded in terms of the small waviness parameter ϵ:

$$\begin{aligned} u &= u^{(0)}(y) + \epsilon u^{(1)}(x, y) + O(\epsilon^2), \\ v &= \epsilon v^{(1)}(x, y) + \epsilon^2 v^{(2)}(x, y) + O(\epsilon^3), \\ p &= p^{(0)}(y) + \epsilon p^{(1)}(x, y) + O(\epsilon^3), \\ f &= \epsilon f^{(1)}(x) + \epsilon^2 f^{(2)}(x) + O(\epsilon^3), \\ g &= \epsilon g^{(1)}(x) + \epsilon^2 g^{(2)}(x) + O(\epsilon^3). \end{aligned} \tag{13}$$

The boundary conditions on the wavy incline $y = \epsilon \sin(\alpha x)$ are also expanded around $\epsilon = 0$, so that at each order of ϵ these boundary conditions are imposed on the mean position of the incline, $y = 0$. This procedure is similarly used for the interface and the free surface conditions. This results in a sequential of boundary-value problems at each order of ϵ. The leading order and the order ϵ problems are:

The $O(1)$ problem:

$$-\frac{\partial p^{(0)}}{\partial x} + G_x + \Delta u^{(0)} = 0, \tag{14}$$

$$-\frac{\partial p^{(0)}}{\partial y} + G_y = 0. \tag{15}$$

The boundary conditions are:

$y = 0$:

$$u^{(0)} = 0. \tag{16}$$

$y = 1$:

$$\|u^{(0)}\| = 0, \tag{17}$$

$$\left\|\frac{\partial u^{(0)}}{\partial y}\right\| = 0, \tag{18}$$

$$-\|p^{(0)}\| = 0. \tag{19}$$

$y = 1 + n$:

$$\frac{\partial u^{(0)}}{\partial y} = 0, \tag{20}$$

$$p^{(0)} = 0. \tag{21}$$

The $O(\epsilon)$ problem:

$$\frac{\partial u^{(1)}}{\partial x} + \frac{\partial v^{(1)}}{\partial y} = 0, \tag{22}$$

$$-\frac{\partial p^{(1)}}{\partial x} + \Delta u^{(1)} = 0, \tag{23}$$

$$-\frac{\partial p^{(1)}}{\partial y} + \Delta v^{(1)} = 0. \tag{24}$$

The boundary conditions are:

$y = 0$:

$$\frac{\partial u^{(0)}}{\partial y} \sin \alpha x + u^{(1)} = 0, \tag{25}$$

$$v^{(1)} = 0. \tag{26}$$

$y = 1$:

$$u^{(0)} \frac{\partial f^{(1)}}{\partial x} = v^{(1)}, \tag{27}$$

$$\|v^{(1)}\| = 0, \tag{28}$$

$$\left\|f^{(1)} \frac{\partial u^{(0)}}{\partial y} + u^{(1)}\right\| = 0, \tag{29}$$

$$\left\|m\left(f^{(1)} \frac{\partial^2 u^{(0)}}{\partial y^2} + \frac{\partial u^{(1)}}{\partial y} + \frac{\partial v^{(1)}}{\partial x}\right)\right\| = 0, \tag{30}$$

$$-\left\|m\frac{\partial p^{(0)}}{\partial y}\right\|f^{(1)}-\|mp^{(1)}\|-2\frac{\partial f^{(1)}}{\partial x}\left\|m\frac{\partial u^{(0)}}{\partial y}\right\|+2\left\|m\frac{\partial v^{(1)}}{\partial y}\right\|-\sigma_1\frac{\partial^2 f^{(1)}}{\partial x^2}=0. \quad [31]$$

$y = 1 + n$:

$$u^{(0)}\frac{\partial \boldsymbol{g}^{(1)}}{\partial x}=v^{(1)}, \quad [32]$$

$$\frac{\partial^2 u^{(0)}}{\partial y^2}g^{(1)}+\frac{\partial u^{(1)}}{\partial y}+\frac{\partial v^{(1)}}{\partial x}=0, \quad [33]$$

$$-\frac{\partial p^{(0)}}{\partial y}\boldsymbol{g}^{(1)}-p^{(1)}-2\frac{\partial \boldsymbol{g}^{(1)}}{\partial x}\frac{\partial u^{(0)}}{\partial y}+2\frac{\partial v^{(1)}}{\partial y}-\sigma_2\frac{\partial^2 \boldsymbol{g}^{(1)}}{\partial x^2}=0. \quad [34]$$

These equations can also be derived rigorously by the domain perturbation method (Joseph 1973). It is noted that these equations are also valid for $\mathrm{Re} = O(\epsilon^n)$, with $n > 1$.

3. SOLUTIONS OF THE BOUNDARY-VALUE PROBLEMS

We are interested in the effects of the wall waviness on the interface and the free surface deformations. These effects can be obtained by solving the boundary-value problems [1]–[12]. At the leading order, the velocity and pressure fields in each layer are given by:

Bottom layer: $0 \leqslant y \leqslant 1$

$$u^{(0)}=\frac{1}{1+2n\zeta}[-y^2+2(1+n\zeta)y], \quad [35]$$

$$p^{(0)}=-\frac{2}{1+2n\zeta}\left(y-n\frac{\zeta}{m}-1\right)\mathrm{ctg}\,\theta; \quad [36]$$

Top layer: $1 \leqslant y \leqslant 1+n$

$$u^{(0)}=\frac{1}{1+2n\zeta}\left[-\frac{\zeta}{m}y^2+\frac{2\zeta}{m}(1+n)y-\frac{\zeta}{m}(1+2n)+1+2n\zeta\right], \quad [37]$$

$$p^{(0)}=-\frac{2}{1+2n\zeta}\frac{\zeta}{m}(y-1-n)\,\mathrm{ctg}\,\theta, \quad [38]$$

where ζ is the density ratio

$$\zeta=\frac{\rho_2}{\rho_1}. \quad [39]$$

The boundary condition [25] for the $O(\epsilon)$ problem suggests that in complex notion, the solution to the $O(\epsilon)$ problem takes the form

$$\Phi(x,y)=\tilde{\Phi}(y)\exp(i\alpha x), \quad (40]$$

with the understanding that only the real part of the right hand side of [40] is taken. The continuity equation then gives

$$\tilde{u}^{(1)}=\frac{i}{\alpha}\frac{\mathrm{d}\tilde{v}^{(1)}}{\mathrm{d}y}, \quad [41]$$

where prime stands for derivative with respect to y. The momentum equations become:

$$0=-i\alpha\tilde{p}^{(1)}+(D^2-\alpha^2)\tilde{u}^{(1)}, \quad [42]$$

$$0=-D\tilde{p}^{(1)}+(D^2-\alpha^2)\tilde{v}^{(1)}, \quad [43]$$

where $D = \mathrm{d}/\mathrm{d}y$. The boundary conditions are

$y = 0$:

$$\alpha D u^{(0)} - D\tilde{v}^{(1)} = 0, \tag{44}$$

$$\tilde{v}^{(1)} = 0. \tag{45}$$

$y = 1$:

$$i\alpha u^{(0)}\tilde{f}^{(1)} = \tilde{v}^{(1)}, \tag{46}$$

$$\|\tilde{v}^{(1)}\| = 0, \tag{47}$$

$$\|\tilde{f}^{(1)} D u^{(0)} + \tilde{u}^{(1)}\| = 0, \tag{48}$$

$$\|m(\tilde{f}^{(1)} D^2 u^{(0)} + D\tilde{u}^{(1)} + i\alpha\tilde{v}^{(1)})\| = 0, \tag{49}$$

$$-\|mDp^{(0)}\|\tilde{f}^{(1)} - \|m\tilde{p}^{(1)}\| - 2i\alpha\tilde{f}^{(1)}\|mDu^{(0)}\| + 2\|mD\tilde{v}^{(1)}\| + \sigma_1\alpha^2\tilde{f}^{(1)} = 0. \tag{50}$$

$y = 1 + n$:

$$u^{(0)} i\alpha\tilde{g}^{(1)} = \tilde{v}^{(1)}, \tag{51}$$

$$\tilde{g}^{(1)} D^2 u^{(0)} + D\tilde{u}^{(1)} + i\alpha\tilde{v}^{(1)} = 0, \tag{52}$$

$$\tilde{g}^{(1)} Dp^{(0)} - \tilde{p}^{(1)} - 2i\alpha\tilde{g}^{(1)} Du^{(0)} + 2D\tilde{v}^{(1)} + \sigma_2\alpha^2\tilde{g}^{(1)} = 0. \tag{53}$$

Eliminating $\tilde{p}^{(1)}$ from [42] and [43], we obtain

$$(D^2 - \alpha^2)^2\tilde{v}^{(1)} = 0. \tag{54}$$

The general solution of [54] is

$$\tilde{v}^{(1)} = c_1 \sin h(\alpha y) + c_2 y \sin h(\alpha y) + c_3 \cos h(\alpha y) + c_4 y \cos h(\alpha y). \tag{55}$$

$\tilde{u}^{(1)}$ and $\tilde{p}^{(1)}$ can be obtained form [41] and [42], respectively. The solution in each layer involves four unknown coefficients, c_j, $j = 1, 2, 3, 4$, for the bottom layer, and we shall use d_j, $j = 1, 2, 3, 4$ for the coefficients in the top layer.

The above solutions are required to satisfy the ten boundary conditions [44]–[53]. This gives a system of algebraic equations for ten unknowns: c_j ($j = 1, 2, 3, 4$), d_j ($j = 1, 2, 3, 4$) and $\tilde{f}^{(1)}$, $\tilde{g}^{(1)}$. A numerical method can be employed to solve the algebraic equations for a given set of parameters.

4. RESULTS

The distortions of the fluid–fluid interface and the fluid–air free surface can be characterized by their amplitude ratios and phase shifts with respect to the wavy incline. To this end, we shall express the leading order interface deformation $f^{(1)}(x)$ and the leading order free surface deformation $g^{(1)}(x)$ as

$$f^{(1)}(x) = A \sin(\alpha x + \gamma), \tag{56}$$

$$g^{(1)}(x) = B \sin(\alpha x + \beta), \tag{57}$$

where A, γ are the amplitude ratio and phase shift for the interface, and B, β are the amplitude ratio and phase shift for the free surface. The amplitude ratios and the phase shifts depend on the wave number α, the ratio of the mean thickness n, the ratio of viscosity m, the ratio of density ζ, the inclination angle θ, the interfacial tension σ_1 and the surface tension σ_2.

The amplitude ratio of the interface, A, is plotted as a function of the wave number α in figure 2, for $n = 1$, $\zeta = 1$, $\sigma_1 = \sigma_2 = 0$, $\theta = 45°$, and various viscosity ratios $m = 0.5$, 1.0, 2.0. $m = 1$ corresponds to the one-fluid configuration. If the top layer is more viscous, $m = 2$, the amplitude of the interface is larger than that for the one-fluid case for long waves with wave number $\alpha < 1.4$, and smaller than the one-fluid case for short waves when $\alpha > 1.4$. This indicates that for this configuration, the viscosity stratification induces a large interface distortion for wave lengths longer

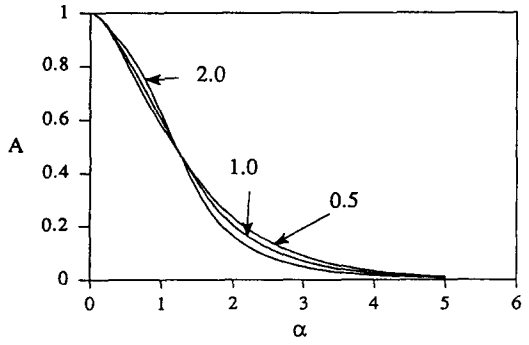

Figure 2. Effect of viscosity stratification m on the interface amplitude A. $n = 1$, $\zeta = 1$, $\theta = 45°$, $\sigma_1 = \sigma_2 = 0$. The number above each curve is the value of corresponding viscosity ratio m. $m = 1$ represents the case of a single fluid.

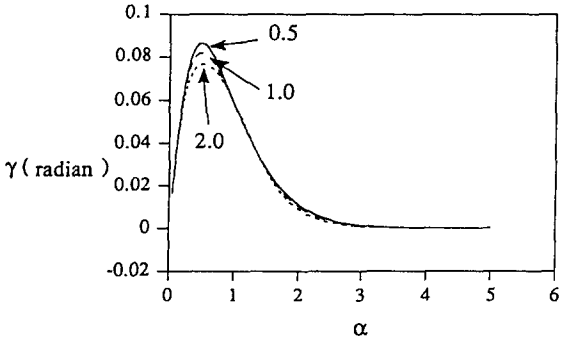

Figure 3. Effect of viscosity stratification on the phase shift of the interface γ. $n = 1$, $\zeta = 1$, $\theta = 45°$, $\sigma_1 = \sigma_2 = 0$. The number above each curve is the value of corresponding viscosity ratio m.

than 4.5 times the lower layer thickness, and suppress the interface distortion for shorter waves. For the opposite configuration with a less viscous top layer, $m = 0.5$, the role of viscosity stratification is reversed: the interface distortion is larger for waves shorter than 4.5 times the lower layer thickness, and smaller for waves longer than that. The interface distortion becomes negligibly small for very short waves, say $\alpha > 4$. When the wavelength is very small compared to the lower layer thickness, its effect on the flow is confined to the vicinity of the incline, and the interface as well as the free surface are not affected. The largest interface distortion, which has the same amplitude as the roughness of the incline ($A = 1$), occurs at very long wave, $\alpha \to 0$.

Effect of viscosity stratification on the phase shift of the interface is plotted in figure 3, for the same parameter set as in figure 2. The phase shift tends to zero as the wave number approaches either zero or infinity. Thus the interface is in phase with the wavy incline for very long and very short waves. A maximum in the phase shift is reached for a wavelength comparable to the lower layer thickness.

Figures 4 and 5 show the interface amplitude ratio and phase shift for density stratified layers, with $n = 1$, $m = 1$, $\sigma_1 = \sigma_2 = 0$, $\theta = 45°$, $\zeta = 0.5$, 1, 2.0. A top-heavy configuration, $\zeta = 2.0$, suppresses interface distortion, although this configuration may suffer the Rayleigh–Taylor instability. On the other hand, a bottom-heavy configuration promotes interface distortion. Top-heavy configuration decreases phase shift, while bottom-heavy configuration increases phase shift.

The thickness ratio of the top layer to the bottom layer, n, has signficant effects on the interface distortion for viscosity stratified layers. In our formulation, the mean thickness of the bottom layer is used as the length scale and the roughness of the inclined plane is assumed to be small compared to this mean thickness. Thus, the mean thickness of the bottom layer is not allowed to approach

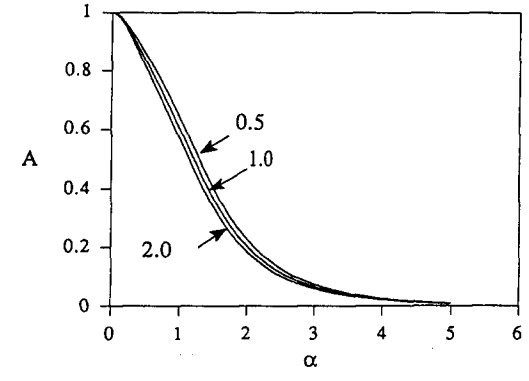

Figure 4. Effect of density stratification on the interface amplitude A. $n = 1$, $m = 1$, $\theta = 45°$, $\sigma_1 = \sigma_2 = 0$. The value of the density ratio ζ is marked above each curve.

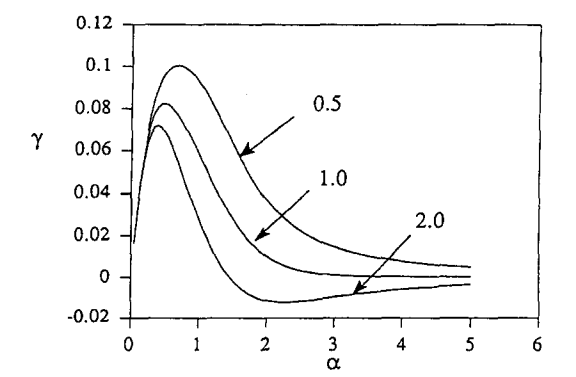

Figure 5. Effect of density stratification on the phase shift of the interface γ. $n = 1$, $m = 1$, $\theta = 45°$, $\sigma_1 = \sigma_2 = 0$. The value of the density ratio ζ is marked above each curve.

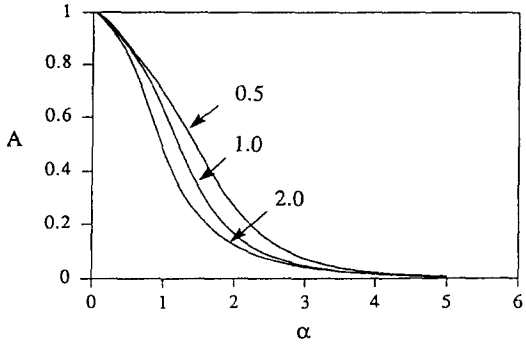

Figure 6. Effect of thickness ratio n on the interface amplitude A. $m = 2$, $\zeta = 1$, $\theta = 45°$, $\sigma_1 = \sigma_2 = 0$. The value of the thickness ratio n is marked above each curve.

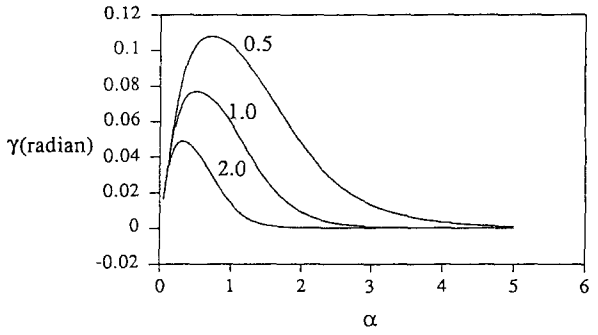

Figure 7. Effect of thickness ratio n on the phase shift of the interface γ. $m = 2$, $\zeta = 1$, $\theta = 45°$, $\sigma_1 = \sigma_2 = 0$. The value of the thickness ratio n is marked above each curve.

zero or even be comparable to that of the roughness of the incline. Varying the thickness ratio n is therefore equivalent to varying the top layer thickness. For an extremely thin bottom layer with a mean thickness comparable to the roughness of the incline, a different length scale has to be used, and the analysis could be very different from the one presented here. Figures 6 and 7 show the interface amplitude ratio and phase shift for the case of a more viscous upper layer, $m = 2$, and various thickness ratios $n = 0.5$, 1, 2. A thicker upper layer, $n = 2$, reduces the amplitude ratio and the phase shift compared to the single layer case, for all wave numbers. A thinner upper layer, $n = 0.5$, on the other hand, always promote the interface distortion as well as phase shift. Similar results are obtained for the case of a less viscous upper layer, $m = 0.5$, as shown in figures 8 and 9. It can be easily verified that for the case of matched densities ($\zeta = 1$), an increase in the thickness ratio n increases the overall mean flow rate, regardless of the direction of viscosity stratification. It is much easier for a fluid element to pass over the small bumps on the incline without significant detour at a higher flow rate than at a lower flow rate (still within the limit that the inertial effects are negligible). Thus the interface deformation is smaller for thick top layers (large values of n) than for thin top layers (small values of n). This effect is robust in the sense that it holds regardless of the direction of viscosity stratification. Similar effects the flow rate has on the free surface for a single film have been discussed by Pozrikidis (1988).

For planar geometry, interfacial tension and surface tension are both restorative forces and they suppress interface and surface distortions. Amplitude ratios of the interface for different values of interfacial tension–surface tension are compared in figure 10 for a viscosity stratified configuration. Large interfacial tension or surface tension are required to see appreciable suppression compared to the case without interfacial and surface tensions. A somewhat surprising result is that for long waves, say $\alpha < 0.7$, the interface amplitude ratio for $(\sigma_1, \sigma_2) = (0, 20)$ is smaller than that for $(\sigma_1, \sigma_2) = (20, 0)$. This means that the surface tension force at the liquid–air free surface is more effective than the interfacial tension force at the liquid–liquid interface in suppressing interface

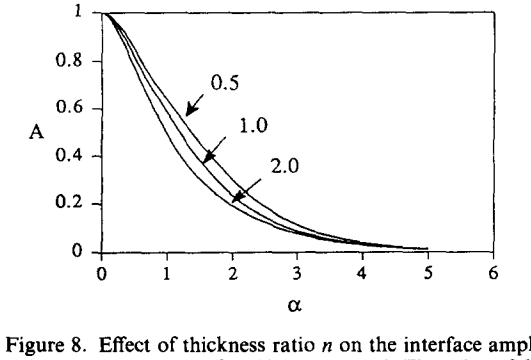

Figure 8. Effect of thickness ratio n on the interface amplitude A. $m = 0.5$, $\zeta = 1$, $\theta = 45°$, $\sigma_1 = \sigma_2 = 0$. The value of the thickness ratio n is marked above each curve.

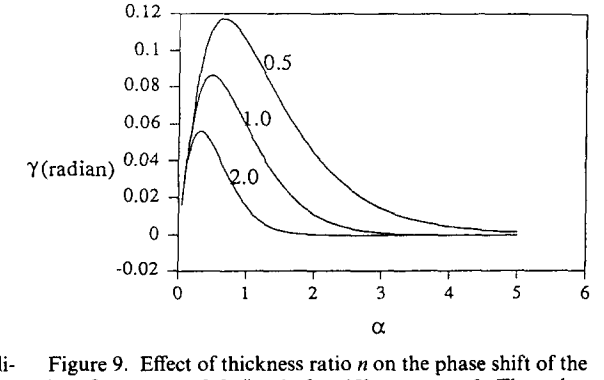

Figure 9. Effect of thickness ratio n on the phase shift of the interface γ. $m = 0.5$, $\zeta = 1$, $\theta = 45°$, $\sigma_1 = \sigma_2 = 0$. The value of the thickness ratio n is marked above each curve.

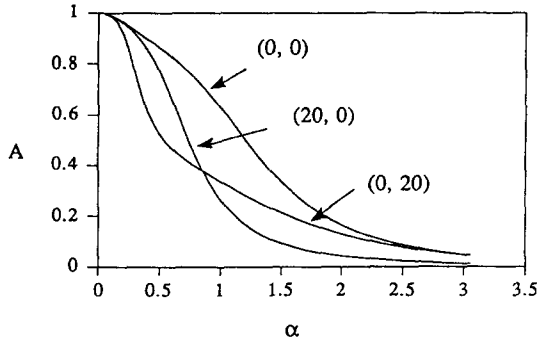

Figure 10. Effect of interfacial and surface tensions on the interface amplitude A. $n = 1$, $m = 2$, $\zeta = 1$, $\theta = 45°$. The values of (σ_1, σ_2) are marked above each curve.

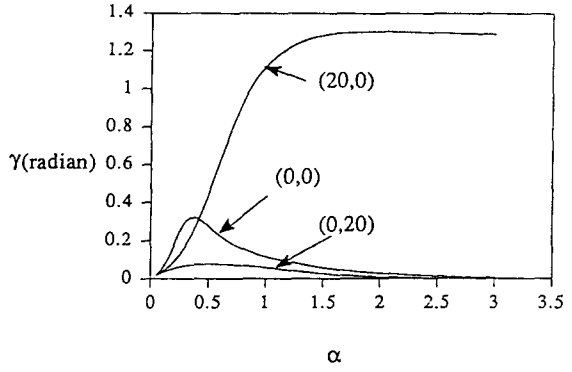

Figure 11. Effect of interfacial and surface tensions on the interface phase shift γ for viscosity stratified layers. $n = 1$, $m = 2$, $\zeta = 1$, $\theta = 45°$. The values of (σ_1, σ_2) are marked above each curve.

deformation for long waves. The opposite is true only for short waves. Phase shift for the same parameter set is plotted in figure 11. Interfacial tension promotes interfacial phase shift while surface tension suppresses interfacial phase shift. An interesting result is that for the case of zero interfacial tension, $\sigma_1 = 0$, and surface tension $\sigma_2 = 20$, the phase shift tends to zero for short waves. On the other hand, if surface tension is zero, and large interfacial tension is present, $\sigma_1 = 20$, the interface will be $\pi/2$ out of phase with the incline for short waves. Qualitatively similar results are obtained when the direction of viscosity stratification is reversed, $m = 0.5$.

Similar results hold for the free surface amplitude ratio and phase shift. The only qualitatively different feature for the free surface distortion is with respect to surface tension variations. Surface tension is always more effective in reducing the free surface amplification, regardless of the wavelength (figure 12). This is in contrast to the interface amplification (figure 10). The effects

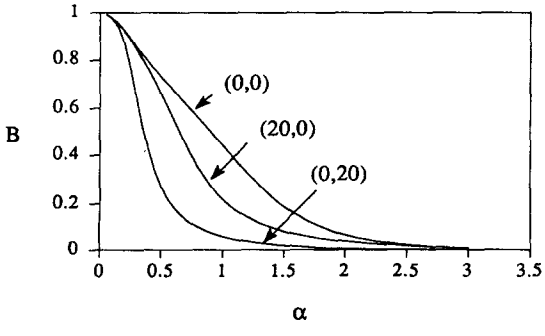

Figure 12. Effect of interfacial and surface tensions on the free surface amplitude B for a viscosity stratified configuration. $n = 1$, $m = 2$, $\zeta = 1$, $\theta = 45°$. The values of (σ_1, σ_2) are indicated above each curve.

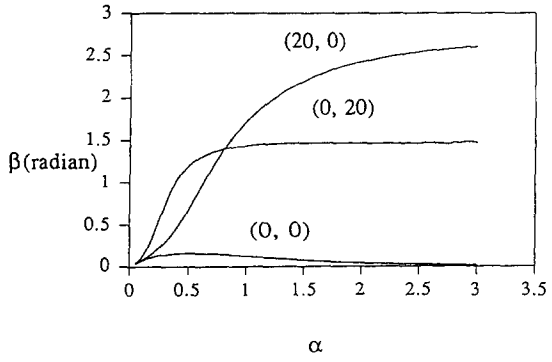

Figure 13. The effect of interfacial and surface tensions on the free surface phase shift β for a viscosity stratified configuration. $n = 1$, $m = 2$, $\zeta = 1$, $\theta = 45°$. The values of (σ_1, σ_2) are indicated above each curve.

of surface tension and interfacial tension are both to increase the phase shift of the free surface (figure 13). Representative shapes of the interface and the free surface have been plotted for two different sets of parameters in figures 14 and 15.

Another useful characterization of the perturbed flow is the wall shear stress distribution. This information is important for certain processes involving mass transfer as discussed in Pozrikidis (1988). The dimensionless wall shear stress, τ_w, scaled with $\eta_1 U/h_1$, where U is the interfacial velocity of the unperturbed flow, is given by

$$\tau_w = 1 + \frac{1}{1+2n\zeta} + \epsilon\left[2\mathrm{RE}(c_2 i \exp(i\alpha x)) - \frac{2}{1+2n\zeta}\sin\alpha x\right], \quad [58]$$

where RE stands for the real part. To the leading order, this dimensionless wall shear stress is independent of the viscosity ratio m. Since the interface velocity of the unperturbed flow is

$$U = \frac{\rho_1 h^2 g \sin\theta}{2\eta_1}(1+2n\zeta), \quad [59]$$

the dimensional wall shear stress is

$$\tau_w^* = (\rho_1 h_1 + \rho_2 h_2) g \sin\theta + \epsilon\left[2\mathrm{RE}(c_2 i \exp(i\alpha x)) - \frac{2}{1+2n\zeta}\sin\alpha x\right]\eta_1 U/h_1. \quad [60]$$

The leading order term on the right hand side of [60] is the result of the balance between gravitational forces and viscous forces for the unperturbed flow, and it is independent of the viscosity of both liquids. Thus the effect of viscosity on the wall shear stress is directly proportional to the amplitude of the inclined wall. The effect of viscosity stratification on the dimensionless wall shear stress τ_w is plotted in figure 16 for $n = 1$, $\zeta = 1$, $\sigma_1 = \sigma_2 = 0$, $\theta = 45°$, $\alpha = 1$, $\epsilon = 0.05$, and $m = 0.1$, 1, 10. It is seen that any viscosity stratification ($m \neq 1$) will increase the maximum perturbation wall shear stress. The mean dimensionless wall shear stress is determined by the

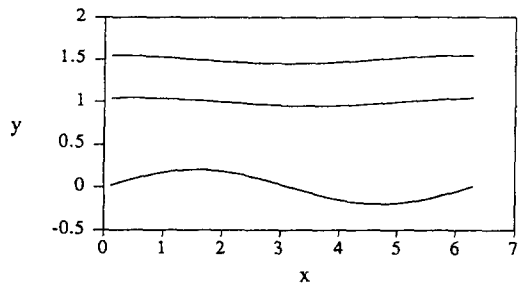

Figure 14. Interface and free surface shapes for $n = 0.5$, $m = 0.1$, $\zeta = 1$, $\theta = 45°$, $\alpha = 1$, $\epsilon = 0.2$, $\sigma_1 = \sigma_2 = 0$.

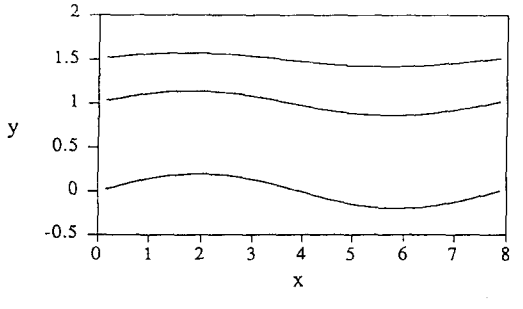

Figure 15. Interface and free surface shapes for $n = 0.5$, $m = 0.5$, $\zeta = 1$, $\alpha = 0.8$, $\theta = 45°$, $\epsilon = 0.2$, $\sigma_1 = \sigma_2 = 0$.

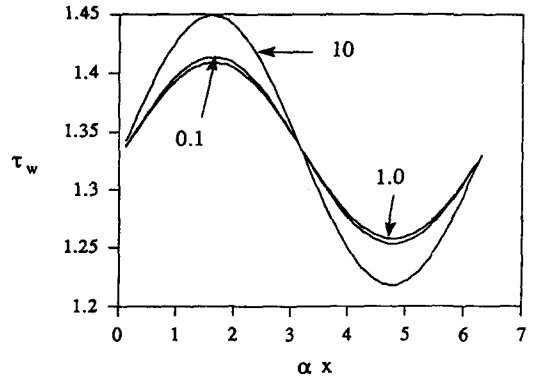

Figure 16. Dimensionless wall shear stress τ_w for viscosity stratified layers $n = 1$, $\zeta = 1$, $\theta = 45°$, $\sigma_1 = \sigma_2 = 0$, $\alpha = 1$, $\epsilon = 0.05$. Viscosity ratio m is marked above each curve.

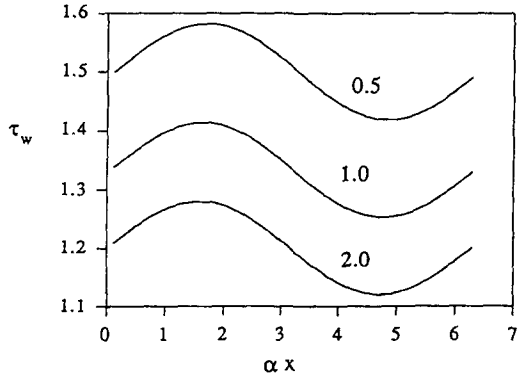

Figure 17. Dimensionless wall shear stress τ_w for density stratified layers $n = 1$, $m = 1$, $\theta = 45°$, $\sigma_1 = \sigma_2 = 0$, $\alpha = 1$, $\epsilon = 0.05$. The density ratio ζ is marked above each curve.

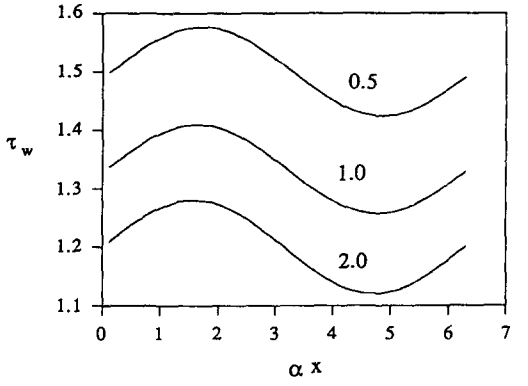

Figure 18. Effect of thickness ratio n on the wall shear stress τ_w for viscosity stratified layers. $m = 0.1$, $\zeta = 1$, $\theta = 45°$, $\sigma_1 = \sigma_2 - 0$, $\alpha = 1$, $\epsilon = 0.05$. The value of n is indicated above each curve.

product $n\zeta$, and decreases as $n\zeta$ is increased. Changes in either n or ζ also have effects on the perturbation wall shear stress, as shown in figures 17–19. Finally, the effects of interfacial tension and surface tension on the wall shear stress are shown in figure 20. Surprisingly, both interfacial and surface tensions increases the perturbaton wall shear stress.

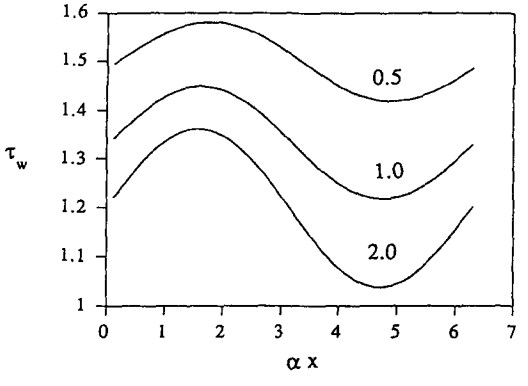

Figure 19. Effect of thickness ratio n on the wall shear stress τ_w for viscosity stratified layers. $m = 10$, $\zeta = 1$, $\theta = 45°$, $\sigma_1 = \sigma_2 = 0$, $\alpha = 1$, $\epsilon = 0.05$. The value of n is indicated above each curve.

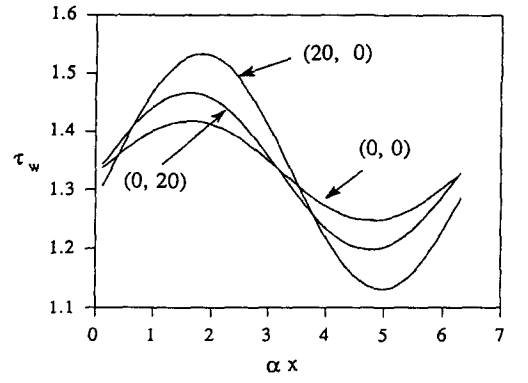

Figure 20. Effect of interfacial and surface tensions on the wall shear stress τ_w for viscosity stratified layers. $n = 1$, $m = 2$, $\zeta = 1$, $\theta = 45°$, $\sigma_1 = \sigma_2 = 0$, $\alpha = 1$, $\epsilon = 0.05$. The values of (σ_1, σ_2) are shown above each curve.

5. CONCLUDING REMARKS

We have studied the steady two-dimensional flow of two liquid films down a slightly wavy sinusoidal plane at low Reynolds numbers. The deformations of both the fluid–fluid interface and the fluid–air free surface are obtained in the leading order in terms of the small amplitude of the wavy incline. The effects of the viscosity stratification on the interface and free surface amplitudes are shown to depend on the wavelength, and the largest amplitude is always achieved for long waves. On the other hand, phase shift reaches a maximum at a wavelength comparable to the lower layer thickness. For density stratified layers, a top-heavy configuration seems to be beneficial for suppressing interface distortion, although this configuration will suffer the Rayleigh–Taylor instability. Larger interface deformation occurs for thin upper layers, and the opposite is true for thick upper layers. Although both interfacial and surface tensions reduce the amplitudes of the interface and the free surface, they all lead to large phase shifts, and increase the perturbation wall shear stress.

The present study is restricted to steady flows. Obviously, the stability of these flows is of great concern. Stability analysis will be considered in the future. Another possible generalization of the present work is to consider finite waviness of the incline. This can be accomplished through numerical simulations.

Acknowledgement—This work is supported by the National Science Foundation and the Xerox Corporation.

REFERENCES

BENJAMIN, T. B. 1957 Wave formation in laminar flow down an inclined plane. *J. Fluid Mech.* **2,** 554–574.

CHEN, K. 1993 Wave formation in the gravity-driven low Reynolds number flow of two liquid films down an inclined plane. *Phys. Fluids A* **5,** 3038–3048.

DASSORI, C. G., DEIBER, J. A. & CASSANO, A. E. 1984 Slow two-phase flow through a sinusoidal channel. *Int. J. Multiphase Flow* **10,** 181–193.

JOO, S. W. & DAVIS, S. H. 1992 Instabilities of three-dimensional viscous falling films. *J. Fluid Mech.* **242,** 529–547.

JOSEPH, D. D. 1973 Domain perturbations: the higher order theory of infinitesimal water waves. *Arch. Rat. Mech. Anal.* **51,** 295–303.

JOSEPH, D. D. & RENARDY, Y. Y. 1993 *Fundamentals of Two-fluids Dynamics*. Springer, New York.

KAO, T. W. 1965a Stability of two-layer viscous stratified flow down an inclined plane. *Phys. Fluids* **8,** 812–820.

KAO, T. W. 1965b Role of the interface in the stability of stratified flow down an inclined plane. *Phys. Fluids* **8,** 2190–2194.

KAO, T. W. 1968 Role of viscosity stratification in the stability of two-layer flow down an incline. *J. Fluid Mech.* **33,** 561–572.

LIN, S. P. 1983 Effects of surface solidification on the stability of multi-layered liquid films. *J. Fluids Engng* **105,** 119–120.

LIN, S. P. & WANG, C. Y. 1985 Modeling wavy film flows. In *Encyclopedia of Fluid Mechanics* (Edited by CHEREMISINOFF, N. P.), Vol. 1, pp. 931–951. Gulf Houston, TX.

LOEWENHERZ, D. S. & LAWRENCE, C. J. 1989 The effect of viscosity stratification on the stability of a free surface flow at low Reynolds number. *Phys. Fluids* **A1(10),** 1686–1693.

POZRIKIDIS, C. 1988 The flow of a liquid film along a periodic wall. *J. Fluid Mech.* **188,** 275–300.

SANTOS, J. M., MELLI, T. R. Q. & SCRIVEN, L. E. 1991 Mechanics of gas–liquid flow in packed-bed contractors. *A. Rev. Fluid Mech.* **23,** 233–260.

TOUGOU, H. 1978 Long waves on a film flow of a viscous fluid down an inclined uneven wall. *J. Phys. Soc. Jap.* **44,** 1014–1019.

WANG, C. Y. 1981 Liquid film flowing slowly down a wavy incline. *AIChE Jl* **27,** 207–212.

WANG, C. Y. 1984 Thin film flowing down a curved surface. *Z. Angew. Math. Phys.* **35,** 533–544.

WANG, C. Y., SEABORG, J. J. & LIN, S. P. 1978 Instability of multi-layered liquid films. *Phys. Fluids* **21,** 1669–1673.

WEINSTEIN, S. J. 1991 Wave propagation in the flow of shear-thinning fluids down an incline. *AIChE Jl* **36,** 1873–1889.

WEINSTEIN, S. J. & KURZ, M. R. 1991 Long-wavelength instabilities in three–layer flow down an incline. *Phys. Fluids* **A3(11),** 2680–2687.

YIH, C. S. 1954 Stability of parallel laminar flow with a free surface. In *Proceedings of the Second U.S. Congress on Applied Mechanics, pp.* 623–628.

YIH, C. S. 1963 Stability of liquid flow down an inclined plane. *Phys. Fluids* **6,** 321–330.